



# Preparation of photocrosslinked spherical hydrogels bearing $\beta$ -cyclodextrin and application in immobilizing microbes to decompose organic pollutants

Hirohito Yamasaki<sup>1</sup> · Yasu-yuki Nagasawa<sup>1</sup> · Kimitoshi Fukunaga<sup>2</sup>

Received: 12 November 2021 / Revised: 18 January 2022 / Accepted: 8 February 2022 / Published online: 1 April 2022  
© The Society of Polymer Science, Japan 2022

## Abstract

A microbe-immobilized support that improves the ability of bacteria to decompose organic pollutants by utilizing the organic inclusion effect of cyclodextrin (CyD) has been developed. Spherical hydrogels (ENTG-*co*-PS $\beta$ CyD) were prepared by photocopolymerization of the polyethylene glycol macromonomer, ENTG, and the polysubstituted photocross-linkable  $\beta$ -CyD macromonomer PS $\beta$ CyD. Then, the optimum composition ratio for use of this hydrogel as a microbe-immobilized support was determined, as were the phenol (PhOH)-removing abilities of PhOH-decomposing bacteria immobilized on this hydrogel. PhOH-degrading bacteria were immobilized on the spherical ENTG-*co*-PS $\beta$ CyD hydrogel to obtain a microbe-immobilized hydrogel. The best microbe-immobilized support was obtained by using a spherical hydrogel with a PS $\beta$ CyD content of approximately 28  $\mu\text{mol g}^{-1}$ , and this resulted in a PhOH-removal rate of 0.76 mg (L h hydrogel g)<sup>-1</sup>. This removal rate was 1.7 times faster, and the amount of free bacteria in the assay medium was 3.6 times lower than the corresponding data obtained using a microbe-immobilized hydrogel without PS $\beta$ CyD. The spherical ENTG-*co*-PS $\beta$ CyD hydrogel had a diameter of 2.9 mm, a moisture content of 63 wt%, a specific gravity of 1.16 g cm<sup>-3</sup> and a Young's modulus of 8.1 MPa. These results suggested that more efficient industrial wastewater treatment technologies must be developed.

## Introduction

Industrial effluents contain many organic pollutants, which must be reduced to levels below the national standards before release into sea or river waters. Chemical, physical and biological methods are available for wastewater treatment. Generally, chemical and physical treatment methods involve high costs, and biological treatments require large facilities, long decomposition times, and discharge of excess sludge. Particularly in densely populated areas, the installation of compact and high-performance industrial wastewater treatment systems is required. Therefore, we decided to develop a microbe-immobilized support that improves the ability of

bacteria to decompose organic pollutants by utilizing the organic inclusion effect of cyclodextrin (CyD) [1–5].

When the synthesized hydrogel biocarrier was used, the CyD component wrapped around the organic contaminants in wastewater and concentrated them in the gel. The immobilized bacteria then decomposed the concentrated organic contaminants. Subsequently, the concentrating function of the hydrogel was recovered. By repeating this cycle, high efficiency was achieved. Furthermore, unlike conventional adsorbents, this process did not require a regeneration treatment process for the carrier.

In this work, we used polyethylene glycol-based photocrosslinked spherical hydrogel KP pearls (Kansai Paint Co., Ltd, Osaka), which have attracted much attention as excellent immobilizing carriers for bacteria [6–12], and ENTG (synthesized using polypropylene glycol, polyethylene glycol, hydroxyethyl acrylate, and isophorone diisocyanate), which was developed in our laboratory and functionalized with multiple substituents of photocopolymerizable groups [13]. The solutions were spheroidized by the calcium alginate method, then photopolymerized to prepare a copolymerized spherical hydrogel (ENTG-*co*-PS $\beta$ CyD). In this study, various spherical hydrogels with

✉ Hirohito Yamasaki  
yamasaki@ube-k.ac.jp

<sup>1</sup> Department of Chemical & Biological Engineering, National Institute of Technology (KOSEN), Ube College, Yamaguchi, Japan

<sup>2</sup> Department of Sustainable Engineering (Chemistry), Graduate School of Science and Engineering, Yamaguchi University, Yamaguchi, Japan

different  $\beta$ -CyD contents were prepared, and the optimum composition ratio was determined by analyzing their physical properties. Then, phenol (PhOH)-decomposing bacteria were immobilized on **ENTG-co-PS $\beta$ CyD** hydrogels, and their PhOH-removing capabilities were evaluated.

We have also developed a PVA-bonded- $\beta$ CyD hydrogel by a formalization reaction between  $\beta$ -CyD and PVA [2]. The crosslinking reaction used to prepare the hydrogel requires heating for 24 h. However, when the hydrogel was obtained using the photocrosslinking reaction described in this paper, the reaction time was as short as 10 min at room temperature, which indicated rapid and facile formation of the hydrogel. Furthermore, to immobilize bacteria in a hydrogel obtained by thermal crosslinking, only a physical adsorption immobilization method can be used. However, for a photocrosslinked hydrogel, a comprehensive immobilization method can be used in addition to physical adsorption. This is because the reaction conditions for hydrogel formation are mild, and the application range is considered wide.

## Materials and methods

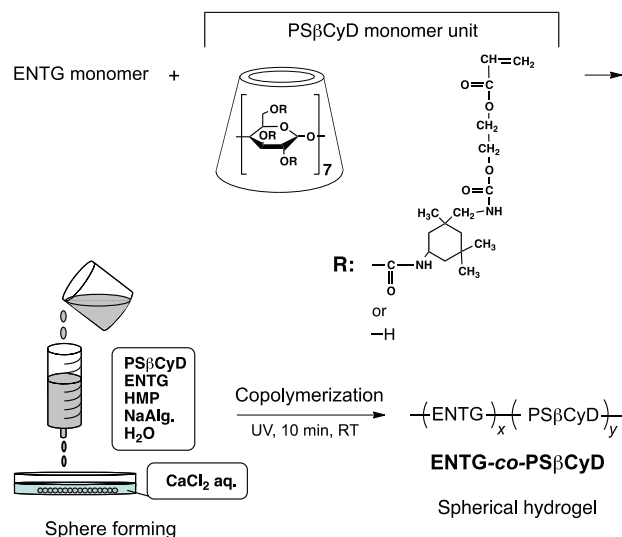
### Experimental apparatus and procedures

#### Reagents

The ENTG macromonomer (ENTG 380), PhOH-degrading bacteria (DC 1002 CG), and PhOH were supplied by Kansai Paint Co., Ltd (Osaka), Novozymes Japan Co., Ltd (Chiba), and Meiwa Plastic Industries, Ltd (Ube), respectively. Sodium alginate (NaAlg, 500 cps) was purchased from Sigma-Aldrich (Tokyo, Japan). The 2-hydroxy-2-methylpropiophenone (HMP) used was purchased from Tokyo Kasei Kogyo (Tokyo, Japan). Dimethyl sulfoxide (DMSO) was used after distillation *in vacuo* and drying over molecular sieves. All other organic and inorganic reagents were of the purest grade and were used as obtained.

#### Preparation and properties of photocrosslinked spherical hydrogels bearing $\beta$ -cyclodextrin (ENTG-co-PS $\beta$ CyD)

The synthesis of the **ENTG-co-PS $\beta$ CyD** spherical hydrogels is outlined in Scheme 1. A 1 wt% aqueous sodium alginate solution (NaAlg. aq.), a fixed amount of ENTG macromonomer, and a small amount of HMP used as a photopolymerization initiator were added to a fixed amount of PS $\beta$ CyD macromonomer in DMSO solution. The mixture was then dropped into a 3% aqueous calcium chloride (CaCl<sub>2</sub> aq.) solution using a syringe with an internal diameter of 2 mm and spheroidized. The resulting spheres were irradiated with UV light for 10 min to prepare the copolymerized **ENTG-co-PS $\beta$ CyD** spherical hydrogels.



**Scheme 1** Preparation of spherical ENTG-co-PS $\beta$ CyD hydrogels bearing  $\beta$ -cyclodextrin by photocrosslinking copolymerization

#### Measurements of moisture content

The moisture on the surfaces of the spherical hydrogels was wiped off, and seven such gels were weighed in the hydrated state ( $W_{\text{wet}}$ ). After drying at 60 °C for 1 day, the dried gels were weighed ( $W_{\text{dry}}$ ), and the moisture content was calculated using the following formula:

$$\text{Moisture content [wt\%]} = (W_{\text{wet}} - W_{\text{dry}}) / W_{\text{wet}} \times 100 \quad (1)$$

#### Measurement of specific gravity

The specific gravities of the spherical hydrogels were measured using a Harvard pycnometer (Sogo Laboratory Glass Works Co., Ltd, Kyoto, Japan). The weight of the pycnometer in the dry state ( $W_0$ ) was measured in advance, and then five spherical hydrous gels were placed in the pycnometer and weighed ( $W_1$ ). Next, distilled water was poured to fill the pycnometer containing the hydrogels and weighed ( $W_2$ ), after which the hydrogels were removed, and the weight of the pycnometer filled with the water was measured ( $W_3$ ). The specific gravity ( $\rho$ ) of water at that temperature was obtained from the literature, and the specific gravity of the hydrogel was calculated using the following equation:

$$\text{Specific gravity[-]} = (W_1 - W_0) / (W_3 - W_2 + W_1 - W_0) \times \rho \quad (2)$$

#### PhOH adsorption experiments

Equilibrium adsorption tests were carried out batchwise by placing 1.0 g of the spherical hydrogels with 5 cm<sup>3</sup> of a 500 mg L<sup>-1</sup> PhOH aqueous solution in a 50 cm<sup>3</sup> Erlenmeyer flask sealed with a polyethylene film and shaking the flask for a fixed time period in a 25 °C chamber at 80 rpm. After 2 and

24 h, the residual liquid and the PhOH clathrate hydrogel were separated by suction filtration, and the concentration of PhOH was determined using a capillary gas chromatograph fitted with a hydrogen flame ionization detector FID-6 (model GC-14A; Shimadzu, Kyoto) employing a Unisole F-200 30/60 column (GL Science Inc., Tokyo). The PhOH concentrating efficiency of the spherical hydrogel was calculated from the mean value obtained by repeating the same procedure three times. The lower limit of detection was  $0.1 \text{ mg L}^{-1}$ .

### Staining test with nitrophenol

To observe the inclusion of PhOH by the  $\beta$ -CyD content in the hydrogels, the hydrogels were dyed with *p*-nitrophenol ( $\text{NO}_2\text{PhOH}$ ), and cross-sections were observed using a digital HF microscope, VHX-1000 (Keyence Co., Osaka). The staining solution was a yellow aqueous solution of  $\text{NO}_2\text{PhOH}$  saturated at  $25^\circ\text{C}$ , and the staining process was performed by immersing four hydrogels in 2 mL of the staining solution for 30 min. The images were recorded 50 times in normal shooting or HDR mode.

### Equipment used and other measurements

A light box model BOX-W 10 (Sunhayato Co., Tokyo, wavelength; 365 nm, intensity;  $19 \mu\text{W cm}^{-2}$ ) was used for UV irradiation during preparation of the spherical hydrogels. For the PhOH inclusion test, a universal shaker NTS-2000 (Tokyo Rikakikai Co., Ltd, Tokyo) was used. Fourier transform infrared (FT-IR) spectra were measured using a JASCO FT/IR-4100 (JASCO Co., Tokyo) spectrophotometer with the KBr method. The compressive strengths of the spherical hydrogels were determined using a tensile and compressive testing machine, STA-1150 (A&D Co. Ltd, Tokyo).

### Examinations for microbe immobilization

#### Preparation of the spherical hydrogel immobilized with PhOH-degrading bacteria medium

Immobilization of the PhOH-degrading bacteria on the hydrogel was performed using an adsorption method. The 1 L liquid medium for adsorption contained 10.49 g of  $\text{K}_2\text{HPO}_4$ , 5.44 g of  $\text{KH}_2\text{PO}_4$ , 0.05 g of  $\text{MgSO}_4 \cdot 7\text{H}_2\text{O}$ , 5.0 mg of  $\text{MnSO}_4 \cdot 4\text{H}_2\text{O}$ , 0.662 mg of  $\text{CaCl}_2 \cdot 2\text{H}_2\text{O}$ , 0.125 mg of  $\text{FeSO}_4 \cdot 7\text{H}_2\text{O}$ , 30 mg of *L*-tryptophan and 2.00 g of  $(\text{NH}_4)_2\text{SO}_4$ . It also contained 7.21 g of glucose, 0.5 g of casamino acid and 0.5 g of PhOH as carbon sources. This liquid medium was called the medium for immobilization [14]. For the PhOH-removal treatment, a medium containing only 0.5 g of PhOH as the carbon source in the above medium composition was used. This was called the medium for measurement.

### Immobilization of microbes onto the spherical hydrogel

PhOH-degrading bacteria were obtained as powders adsorbed on sawdust. Sterile saline (100 mL) and bacterial cells (10 g) were mixed, filtered through gauze, separated from sawdust, and then added to 200 mL of sterile immobilization medium. The medium was preincubated for 2 days.

The medium ( $500 \text{ cm}^3$ ) for immobilization and 50 g of the spherical hydrogel were placed in a pressure-resistant container and sterilized in an autoclave at  $121^\circ\text{C}$  for 20 min. The sterilized spherical hydrogel was placed in a net and charged into a bubble column reactor made of PET bottles along with  $50 \text{ cm}^3$  of the precultured solution containing PhOH-degrading bacteria and the sterilized fixed medium [1,15]. The reactor was covered with a wrap film and incubated for 1 month at room temperature in batches with a constant water content. PhOH-degrading bacteria were immobilized by physical adsorption.

In this study, the original carrier without immobilized PhOH-degrading bacteria is described as a hydrogel, and the carrier containing immobilized PhOH-degrading bacteria is described as a microbe-immobilized support.

### PhOH-removal treatment

A microbe-immobilized support and  $500 \text{ cm}^3$  of the sterilized medium for measurement were charged into a bioreactor, and the reactor was covered with a wrap film. At predetermined time intervals, 1 mL of the culture medium (treated water) was drawn using a syringe. The treated water was sterilized on a chromatographic disk (13 A, water system,  $0.2 \mu\text{L}$ , GL Science Co., Ltd, Tokyo) and subjected to gas chromatographic analysis.

### Other measurements for the microbe-immobilized support

An ultraviolet/visible (UV-Vis) spectrophotometer, IUU-1240 (Shimadzu Co., Kyoto), was used to measure the amount of free bacteria. The surface properties of the immobilized support were studied using optical microscopy with a VH-8000 digital microscope (Keyence Co., Osaka).

## Results and discussion

### Preparation and properties of photocrosslinked ENTG-co-PS $\beta$ CyD

#### Preparation

Eleven types of spherical hydrogels with different PS $\beta$ CyD and ENTG macromonomer ratios were obtained by changing the charging ratio every 5 wt% using a PS $\beta$ CyD

**Table 1** Preparation and properties of spherical ENTG-*co*-PS $\beta$ CyD hydrogels obtained from photocrosslinking reactions and their performance in phenol adsorption

Run	Preparation		Physical properties				Phenol adsorption <sup>b</sup>	
	Weight ratio of PS $\beta$ CyD in feed (wt%)	PS $\beta$ CyD content <sup>a</sup> in hydrogel ( $\mu\text{mol g}^{-1}$ )	Young's modulus (MPa)	Diameter (mm $\phi$ )	Moisture content (wt%)	Specific gravity ( $\text{g cm}^{-3}$ )	Concentrating efficiency <sup>c</sup>	
							2 h (%)	24 h (%)
1	100	196	47	2.7	37	1.09	64	76
2	95	97	29	3.4	48	–	62	66
3	90	86	24	3.2	45	–	61	70
4	85	67	19	3.3	51	–	61	71
5	80	54	16	3.1	52	–	67	83
6	75	54	14	3.1	54	1.09	65	74
7	70	37	9.6	3.0	59	–	65	81
8	65	28	8.1	2.9	63	1.16	57	67
9	60	18	1.3	3.4	67	–	68	69
10	55	18	1.4	3.0	72	1.15	58	69
11	50	14	1.0	3.5	72	–	63	66
12	45	16	1.4	4.3	75	–	58	60
13	33	11	0.7	3.9	74	1.06	53	63
14	10	1	0.3	4.7	82	1.04	54	55
15	0	0	0.7	4.2	78	1.04	57	57

<sup>a</sup>Measured by Fourier transform infrared spectroscopy

<sup>b</sup>Adsorption was carried out by placing the spherical ENTG-*co*-PS $\beta$ CyD hydrogel (1.0 g) and 500 mg L<sup>-1</sup> phenol aqueous solution (5 cm<sup>3</sup>) in a 50 mL Erlenmeyer flask at 25 °C and shaking at 80 rpm for 2 h and/or 24 h

<sup>c</sup>Concentrating efficiency (%) was calculated from the difference between phenol concentrations before and after adsorption

charging ratio of 95–45 wt% (Table 1, runs 2–12). Because a change in the charging ratio caused minor changes in the properties of the hydrogel (45 wt% or less), hydrogels with 33 wt% (Table 1, run 13) and 10 wt% (Table 1, run 14) were prepared. Hydrogels of the PS $\beta$ CyD homopolymer (Table 1, run 1) [13] and the ENTG homopolymer (Table 1, run 15) were prepared as reference standards.

The approximate amounts of PS $\beta$ CyD in the spherical hydrogels were calculated from the area ratios of the different ether absorption peaks in the FT-IR spectra of  $\beta$ -CyD and ENTG. The FT-IR spectra of ENTG-*co*-PS $\beta$ CyD (Table 1, run 8), the PS $\beta$ CyD homopolymer (Table 1, run 1), and the ENTG homopolymer (Table 1, run 15) are shown in Fig. 1. The figure is expanded in the 700–900 cm<sup>-1</sup> range in which the specific ether peaks of PS $\beta$ CyD and ENTG appeared, and the absorption peaks for the cyclic ethers from  $\beta$ -CyD and the linear ethers from ENTG appeared at 750–800 cm<sup>-1</sup> and 820–880 cm<sup>-1</sup>, respectively. The ether peak derived from  $\beta$ -CyD was thought to have shifted to shorter wavelengths because of the presence of electron-withdrawing groups around it. A calibration curve was prepared by mixing the PS $\beta$ CyD homopolymer with the ENTG homopolymer in an arbitrary ratio and using the peak area ratios appearing in the wavenumber ranges

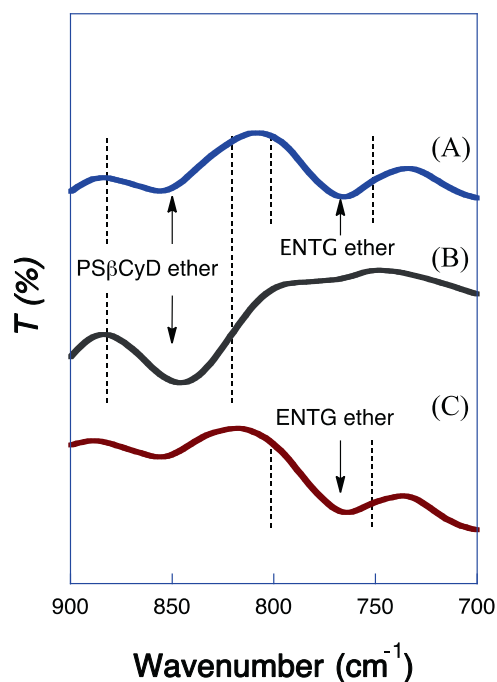


**Fig. 1** FT-IR spectra of **A** ENTG-*co*-PS $\beta$ CyD (Table 1, run 8), **B** PS $\beta$ CyD homopolymer (Table 1, run 1) and **C** ENTG homopolymer (Table 1, run 15) in the wavenumber range 700–900 cm<sup>-1</sup>

750–800 and 820–880  $\text{cm}^{-1}$ , which were due to the respective ethers. The approximate amount of PS $\beta$ CyD contained in the spherical hydrogel increased with increasing charging composition ratio.

The PS $\beta$ CyD content, Young's modulus (compressive strength), diameter, moisture content, and specific gravity of the spherical hydrogel obtained are shown in Table 1.

### Properties

There were only minor differences in the diameters of the prepared hydrogels, but the hydrogel with a high proportion of ENTG had a slightly larger sphere size than the others owing to its high moisture content.

The moisture content was determined by comparing the weights of the hydrogels under dry and wet conditions. The hydrogel containing 90 wt% or more of the charged PS $\beta$ CyD component, that is,  $\geq 86 \mu\text{mol g}^{-1}$  of PS $\beta$ CyD content, had a moisture content of less than 50 wt%. Because the moisture content of the ENTG homopolymer hydrogel was approximately 80 wt%, it was considered to be inappropriate for bacterial growth. In contrast, a hydrogel containing 55 wt% or less of the PS $\beta$ CyD component, that is,  $\leq 18 \mu\text{mol g}^{-1}$  of PS $\beta$ CyD content, had a moisture content of 70 wt% or more and was considered to provide an excellent environment for bacterial growth. These results suggested that an increase in the ENTG content was related to an increase in the moisture content of the hydrogel and that copolymerization of the ENTG macromonomer provided a suitable environment for bacterial growth.

The specific gravity increased with increasing PS $\beta$ CyD content and was  $1.16 \text{ g cm}^{-3}$  in the 65 wt% hydrogel (Table 1, run 8) compared to  $1.04 \text{ g cm}^{-3}$  in the ENTG homopolymer hydrogel (Table 1, run 15). The 75 wt% hydrogel (Table 1, run 6) had a specific gravity of  $1.09 \text{ g cm}^{-3}$ , which was lower than that of the 65 wt% hydrogel. Thus, the 75 wt% hydrogel had a sparser structure than the 65 wt% hydrogel and was thought to be brittle.

Figure 2 shows the changes in the Young's modulus and the moisture content resulting from the PS $\beta$ CyD content in several ENTG-co-PS $\beta$ CyD hydrogels. As the content of PS $\beta$ CyD was increased, the Young's modulus increased, and the moisture content decreased. Thus, the hydrogel with a high content of PS $\beta$ CyD ( $54 \mu\text{mol g}^{-1}$  or more) had a high Young's modulus of 16–47 MPa; it was hard to deform and therefore brittle and easy to crack. Here, the moisture content was less than 55 wt%. As the content of PS $\beta$ CyD decreased, the Young's modulus of the hydrogel decreased, and it became softer. The spherical hydrogel containing less than  $20 \mu\text{mol g}^{-1}$  PS $\beta$ CyD showed a constant Young's modulus of approximately 1 MPa and a moisture content of 65 wt% or more.

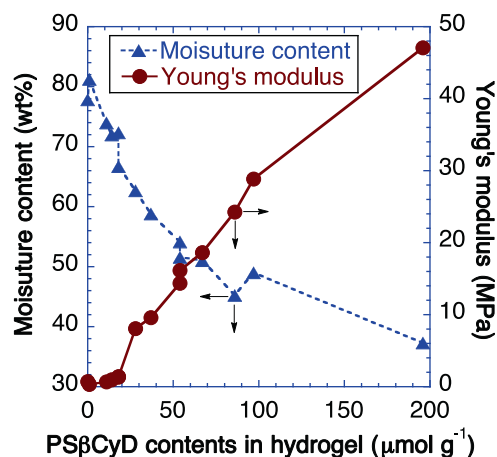


**Fig. 2** Relationships between the Young's modulus and the moisture content with the PS $\beta$ CyD content in spherical ENTG-co-PS $\beta$ CyD hydrogels

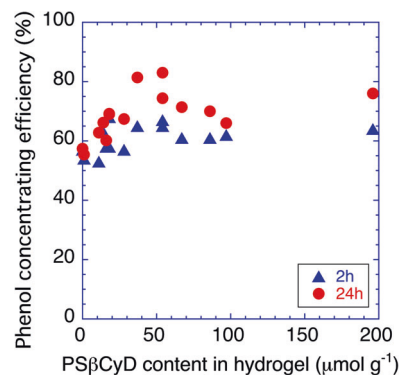


**Fig. 3** Plots of phenol concentrating efficiency for PS $\beta$ CyD content in spherical ENTG-co-PS $\beta$ CyD hydrogels;  $\blacktriangle$ ; after 2 h,  $\bullet$ ; after 24 h. Adsorption was carried out by placing spherical ENTG-co-PS $\beta$ CyD hydrogels (1.0 g) and  $500 \text{ mg L}^{-1}$  phenol aqueous solution ( $5 \text{ cm}^3$ ) in a  $50 \text{ cm}^3$  Erlenmeyer flask at  $25^\circ\text{C}$  and shaking at 80 rpm for 2 h and/or 24 h

### Adsorption of PhOH

To confirm the changes in chemical and physical adsorption capacity of the spherical hydrogel caused by introduction of the  $\beta$ -CyD component, the PhOH inclusion ratio was studied. In this study, residual PhOH concentrations were measured at 2 h with a  $500 \text{ mg L}^{-1}$  aqueous PhOH solution and at 24 h to observe the adsorption equilibrium (Fig. 3). The PhOH concentrating efficiencies after 2 h and 24 h gradually increased with increasing PS $\beta$ CyD content. The PhOH concentration ratio was higher after 24 h than after 2 h. However, the difference in the PhOH concentration effect for the hydrogel rich in the ENTG component between 2 and 24 h was very small. This was due to a decrease in the content of the  $\beta$ -CyD component in the hydrogel, which resulted in a decrease in its ability to concentrate PhOH. In addition, it is suggested that the

complex three-dimensional network structure formed by ENTG restricted access to the  $\beta$ CyD residue in the core of the hydrogel by PhOH. Hydrogels with PS $\beta$ CyD contents of 35  $\mu\text{mol g}^{-1}$  or more exhibited effective concentration of PhOH and levels of 70–80% after 24 h.

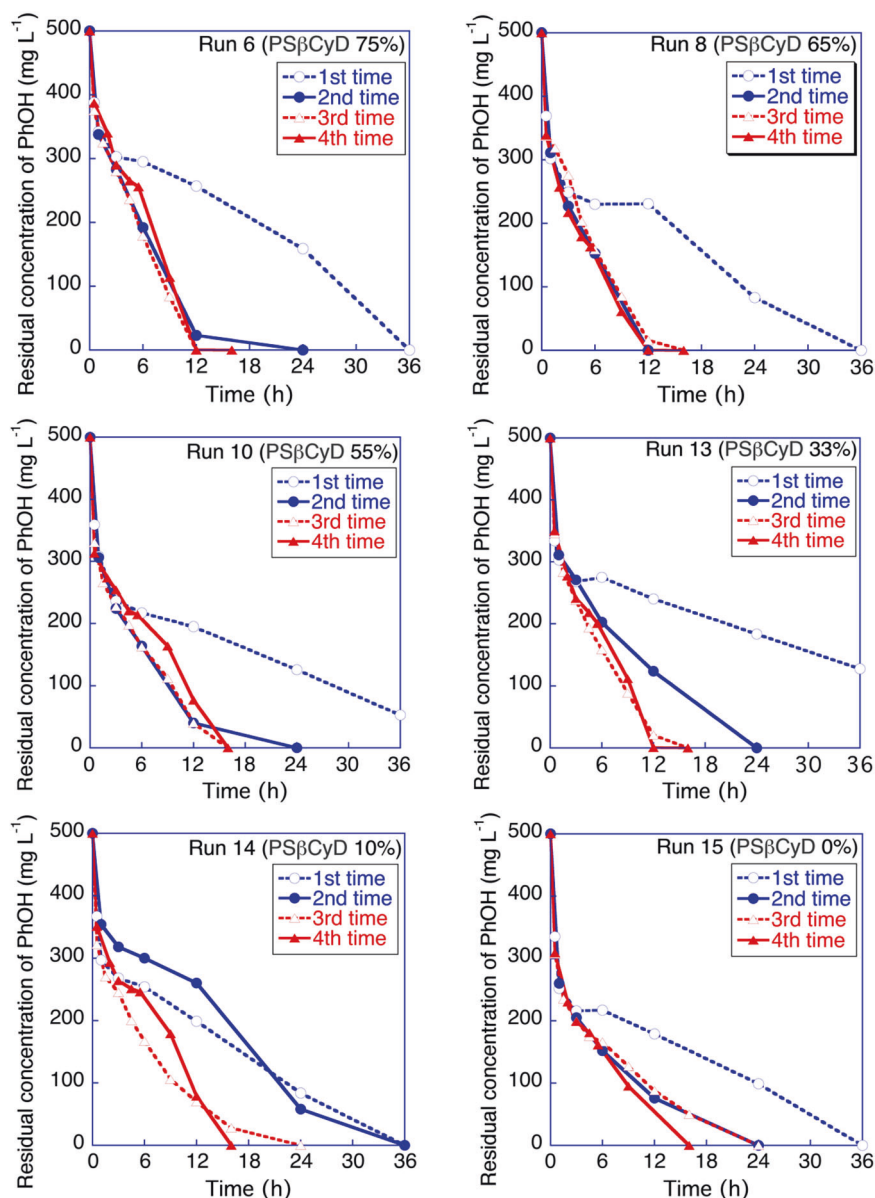
### PhOH-removal by spherical hydrogel-immobilized PhOH-degrading bacteria

For immobilization of the PhOH-degrading bacteria and measurements of PhOH-removal rates, spherical hydrogels with 75% (Table 1, run 6), 65% (Table 1, run 8), 55% (Table 1, run 10), 33% (Table 1, run 13), 10% (Table 1, run 14), and 0% (Table 1, run 15) PS $\beta$ CyD charging

composition ratios were used. Hydrogels containing 80% or more PS $\beta$ CyD were excluded from this study because they were hard, brittle, and difficult to form into spheres. To prevent the growth of bacteria other than PhOH-degrading bacteria, 500  $\text{mg L}^{-1}$  PhOH was added to the immobilizing medium. After 3 days of preincubation, the cell masses were 13.75  $\text{g L}^{-1}$  (wet) and 7.43  $\text{g L}^{-1}$  (dry). In addition, the test was carried out 10 to 14 days before measurement of the removal rate, in a state in which no carbon source was provided and no PhOH remained inside the microbe-immobilized support.

Figure 4 shows the results of PhOH-removal tests using immobilized PhOH-degrading bacteria containing different proportions of the PS $\beta$ CyD component. In the first run, the

**Fig. 4** Time plots for repetition of phenol removal by spherical ENTG-co-PS $\beta$ CyD hydrogel-immobilized phenol-degrading bacteria. Phenol removal tests were carried out batchwise with the obtained immobilized biocatalysts in model wastewater containing 500  $\text{mg L}^{-1}$  phenol



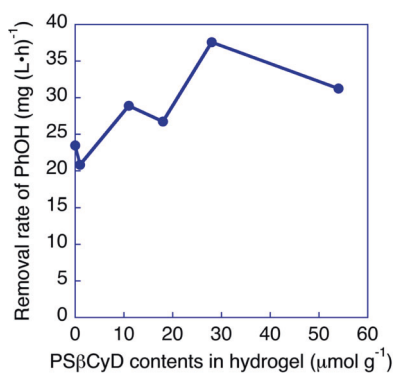


**Fig. 5** Average rate for phenol removal by the spherical ENTG-co-PS $\beta$ CyD hydrogel-immobilized phenol-degrading bacteria. Phenol removal tests were carried out batchwise with the obtained immobilized biocatalysts in model wastewater containing 500 mg L<sup>-1</sup> phenol

processing speed was slow, and a processing time of 36 h or more was required. This was justified by the fact that the time used for immobilization of the bacterial cells on the support was short, so the bacteria were not sufficiently acclimatized by then. After the second run, as the PS $\beta$ CyD content increased, the completion time for PhOH-removal gradually decreased. For all of the microbe-immobilized supports, the decrease in residual PhOH concentration was very rapid for up to 3 h after the start of the test and then became slightly slower. However, the residual PhOH concentration decreased more linearly when using the immobilized hydrogel having a higher PS $\beta$ CyD content, and it reached the measurement limit of the GC within a shorter time. Thus, the microbe-immobilized hydrogel with high PS $\beta$ CyD content seemed to have improved substance permeability and showed a linear decrease in the residual PhOH concentration due to the inclusion effect of  $\beta$ -CyD, and the molecular structure of bulky PS $\beta$ CyD was brought about by  $\beta$ -CyD and the phorone groups. When the PhOH-removal test was repeated, it was equally efficient. It is thought that the PhOH included in the  $\beta$ -CyD residue in the microbe-immobilized hydrogel was decomposed by the bacteria, which regenerated the inclusion function of the  $\beta$ -CyD residue and allowed inclusion of another PhOH.

Figure 5 shows the relationships among the mean PhOH-removal rates for three batches (second to fourth) after completion of acclimation and the contents of PS $\beta$ CyD in the microbe-immobilized hydrogels. The removal rates for the ENTG microbe-immobilized hydrogel and the PS $\beta$ CyD-containing microbe hydrogel were 23 and 21–38 mg h<sup>-1</sup>, respectively. The mean PhOH-removal rate for the microbe-immobilized hydrogel containing PS $\beta$ CyD concentrations above 11  $\mu\text{mol g}^{-1}$  increased with increasing PS $\beta$ CyD content. The best results were obtained with a microbe-immobilized hydrogel containing 28  $\mu\text{mol g}^{-1}$  PS $\beta$ CyD (Table 1, run 8), which showed a PhOH-removal rate that was approximately 1.7 times faster than that of the ENTG

microbe-immobilized hydrogel (Table 1, run 15; PS $\beta$ CyD content: 0  $\mu\text{mol g}^{-1}$ ).

The high performance with PhOH was derived from its basic structure as a monoxygenate, which is first converted to catechols and hydroquinones by microorganisms [16]. Therefore, catechols and hydroquinones can be extruded from the inside of CyD instead of PhOHs [17]. Next, the catechols and hydroquinones are oxidized through an aromatic ring cleavage to carbon dioxide and water. In doing so, the CyD cavity is regenerated and can take up a new PhOH substrate.

### Amounts of free bacteria in the assay medium

One of the problems with biological treatment is the discharge of excess sludge. The solution to this problem is to minimize the number of free bacteria. Therefore, the amount of free bacteria in the PhOH-removal medium was monitored by measuring the turbidity at 580 nm with a UV-Vis spectrophotometer. The following four microbe-immobilized hydrogels containing PS $\beta$ CyD were used: 75% PS $\beta$ CyD (Table 1, run 6), 65% PS $\beta$ CyD (Table 1, run 8), 55% PS $\beta$ CyD (Table 1, run 10), and 0% PS $\beta$ CyD (Table 1, run 15). The time courses for the residual PhOH concentrations and free cell masses are shown in Fig. 6A, B, respectively. All microbe-immobilized hydrogels containing PS $\beta$ CyD showed flat turbidity readings of 0.15–0.2 absorbance units at 580 nm for cuvettes with a 1 cm path length, and the quantity of free bacterial cells in the medium was constantly low.

The turbidity peaks for the microbe-immobilized hydrogels containing PS $\beta$ CyD (55%, 65%, and 75%) were highest on the 1st day, which was in good agreement with the times when the residual PhOH concentration was almost 0 mg L<sup>-1</sup>. In contrast, in the microbe-immobilized hydrogel without PS $\beta$ CyD (0%), the turbidity peak increased rapidly from the 2nd to the 3rd day and reached 0.71 absorbance units. From a comparison of the turbidity peaks for microbe-immobilized hydrogels with and without PS $\beta$ CyD, it was determined that the microbe-immobilized hydrogels containing PS $\beta$ CyD (55–75%) caused 2.5- to 3.6-fold reductions in the generation of free bacterial cells. The turbidity of the microbe-immobilized hydrogel without PS $\beta$ CyD (0%) drastically decreased after the third day, suggesting that the bacterial cells rapidly died out when PhOH, which was the carbon source in the medium, was consumed. In contrast, for the microbe-immobilized hydrogels containing PS $\beta$ CyD, the amount of free bacterial cells remained constant at 50–75% of the peak value even after one week. Thus, it was suggested that the microbe-immobilized hydrogels containing PS $\beta$ CyD mainly degraded PhOH with the immobilized cells in the hydrogel, whereas the microbe-immobilized hydrogel without

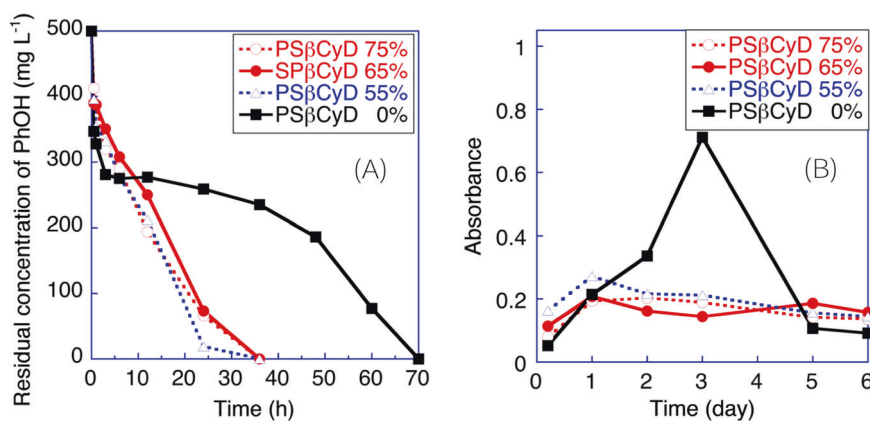


**Fig. 6** Time course for turbidity due to free bacteria in the phenol removal medium. **A** Phenol residual concentration, **B** Turbidity as a free cell mass. Phenol removal tests were carried out batchwise with the obtained immobilized biocatalysts in model wastewater containing

500 mg L<sup>-1</sup> phenol. The changes in phenol concentration and free cell mass were determined by gas chromatographic analysis and an ultraviolet/visible spectrophotometer, respectively

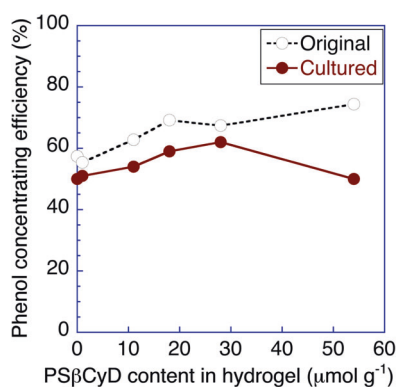


**Fig. 7** Comparison of phenol concentrating performance for the spherical hydrogel regenerated after 8 months with the original performance. Adsorption was carried out by placing the spherical ENTG-*co*-PSβCyD hydrogels (1.0 g) and 500 mg L<sup>-1</sup> phenol aqueous solution (5 cm<sup>3</sup>) in a 50 cm<sup>3</sup> Erlenmeyer flask at 25 °C and shaking at 80 rpm for 24 h. The concentrating efficiency (%) was calculated from the difference between phenol concentrations before and after adsorption

PSβCyD mainly degraded PhOH with free cells. The microbe-immobilized hydrogel containing PSβCyD was found to provide an excellent environment for propagation of bacterial cells and reduction of excess sludge.

### PhOH concentrating performance of a spherical hydrogel regenerated after 8 months of usage

Degradation of a spherical hydrogel was investigated after 8 months of usage. A PhOH inclusion test was carried out in a 500 mg L<sup>-1</sup> aqueous PhOH solution for 24 h to compare its physical and chemical effects on the spherical hydrogel before and after use as a microbe-immobilized support. The spherical hydrogel was used after sterilizing the immobilized bacterial cells in an autoclave (121 °C,

20 min). As shown in Fig. 7, compared with the original spherical hydrogel, most of the microbe-immobilized hydrogels maintained a sufficient PhOH concentration. For example, a hydrogel with a PSβCyD content of 28 μmol g<sup>-1</sup> (Table 1, run 8) retained 93% of its inclusion ability. This result confirmed that the residual β-CyD in the hydrogel was not decomposed by bacteria. In contrast, the hydrogel exhibiting the highest content of PSβCyD (54 μmol g<sup>-1</sup>) (Table 1, run 6) retained 70% of its inclusion ability and showed higher degradation efficiency than the other spherical hydrogels. Because this hydrogel had a high Young's modulus (14 MPa, Table 1, run 6), it became brittle after long-term use, and the inside of the hydrogel was cavitated by a granule, as will be described later. Considering both the average PhOH-removal time and the durability, it was found that the hydrogel with a PSβCyD content of 28 μmol g<sup>-1</sup> (Table 1, run 8) was the best microbe-immobilizing support.

### Microscopic observation of a spherical hydrogel

Microscopic images of the surfaces and a cross-sections of prepared spherical hydrogels are shown in Fig. 8. The hydrogel composed of ENTG homopolymers (PSβCyD 0%; Table 1, run 15) exhibited continuous and smooth structures on both the surfaces and cross-sections. However, in hydrogels containing PSβCyD (55%; Table 1, run 10, 65%; Table 1, run 8, 75%; Table 1, run 6), the surfaces and cross-sections became rugged and coarse in proportion to the PSβCyD content, and the cross-sections indicated that small grains had gathered. This structure showed an increased number of cavities in the spherical hydrogels and improved molecular permeabilities.

A micrograph of a microbe-immobilized hydrogel taken after four months of usage is shown in Fig. 9. There was



**Fig. 8** Enlarged pictures of surfaces and transverse images for original spherical PS $\beta$ CyD-*co*-ENTG hydrogels

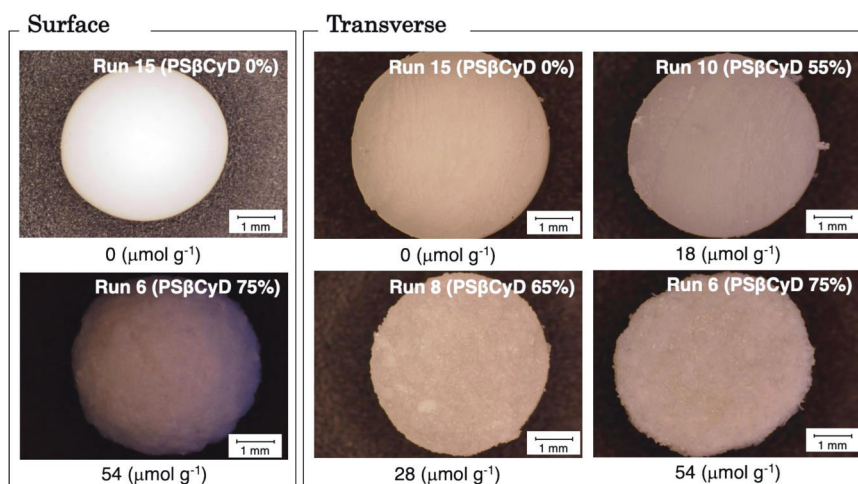
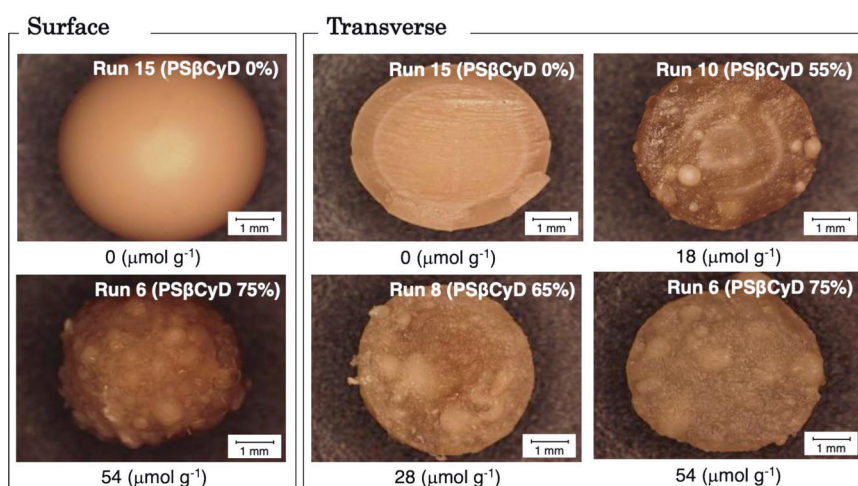


**Fig. 9** Enlarged pictures of surfaces and transverse images for the spherical ENTG-*co*-PS $\beta$ CyD hydrogel-immobilized phenol-degrading bacteria after 4 months of use



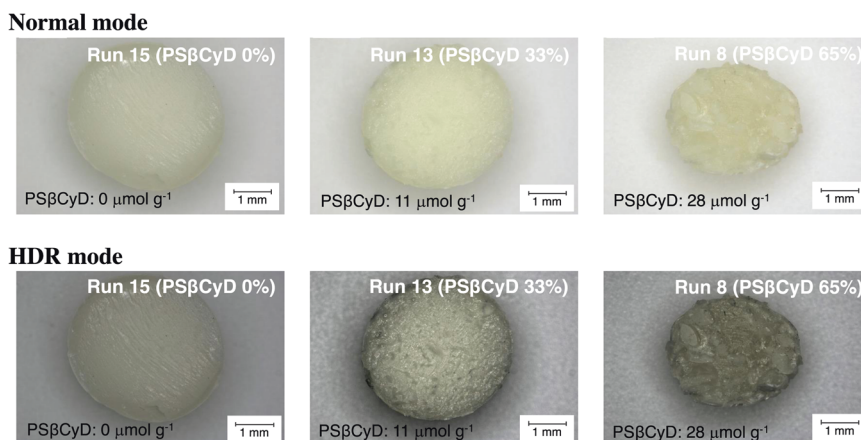
appreciable retention of spherical shapes in all microbe-immobilized hydrogels. In these pictures, the microbe-immobilizing hydrogels containing PS $\beta$ CyD (55%, 65%, and 75%) had many white masses of approximately 0.2–0.5 mm $\phi$  on their surfaces and cross-sections. These masses were not observed in the original spherical hydrogels and were therefore considered to be granular masses composed of bacterial cells. In contrast, no granules were observed in microbe-immobilized hydrogels with PS $\beta$ CyD contents of less than 18  $\mu\text{mol g}^{-1}$ . This may be because in the microbe-immobilized hydrogels rich in the ENTG component, there was no space to form granules due to the dense continuous gel network structure. Thus, PhOH, which was the source of bacteria and nutrients, could not sufficiently penetrate this hydrogel.

### Material permeability

A dyeing test using a yellow NO<sub>2</sub>PhOH aqueous solution was carried out to visually confirm penetration of PhOH

into the hydrogels. The degree of inclusion of *p*-NO<sub>2</sub>PhOH into  $\beta$ -CyD was approximately the same as that of PhOH [17]. Therefore, it was assumed that PhOH reached the point at which the hydrogel was stained yellow in the dyeing test. A micrograph is shown in Fig. 10. Because the light source was a halogen lamp, the yellow color of the hydrogel could hardly be observed. Therefore, a high dynamic range (HDR) image is provided in the lower part of this figure, and a normal observation image is provided in the upper part. The central part of the spherical ENTG-*co*-PS $\beta$ CyD hydrogel containing a large amount of PS $\beta$ CyD was dyed yellow, and the inclusion effect of  $\beta$ -CyD appeared clearly. In the hydrogel with a small amount of the PS $\beta$ CyD component, only the outer peripheral part was dyed thinly, and the one without PS $\beta$ CyD (PS $\beta$ CyD 0%; 0  $\mu\text{mol g}^{-1}$ ) was hardly dyed, and only the surface showed color. The above results confirmed that the inclusion effect of the ENTG-*co*-PS $\beta$ CyD hydrogel was directly proportional to the  $\beta$ -CyD content in the hydrogel.

**Fig. 10** Enlarged transverse pictures of spherical hydrogels with PS $\beta$ CyD 65% (Table 1, run 8), PS $\beta$ CyD 33% (Table 1, run 13) and PS $\beta$ CyD 0% (Table 1, run 15) after dyeing tests with aqueous nitrophenol for 30 min (photographic modes: the upper row shows normal images, the lower row shows High Dynamic Range images)



## Conclusion

The ENTG-co-PS $\beta$ CyD spherical hydrogel obtained by photocrosslinking polymerization of a PS $\beta$ CyD macromonomer and an ENTG macromonomer was found to be a carrier for an immobilized biocatalyst capable of carrying out efficient wastewater treatment. It effectively repeated a PhOH decomposition cycle carried out by immobilized PhOH-decomposing bacteria for treatment of wastewaters containing PhOH. In addition, comprehensive evaluations of PhOH concentration by the prepared photocopolymerized spherical hydrogels, the physical durability of hydrogels during long-term usage, and the activities of the immobilized PhOH-degrading bacteria indicated that the hydrogel (Table 1, run 8) with a PS $\beta$ CyD content of approximately 28  $\mu\text{mol g}^{-1}$  (PS $\beta$ CyD content 65 wt%) was most effective. The hydrogel had a diameter of 2.9 mm, a moisture content of 63 wt%, a specific gravity of 1.16  $\text{g cm}^{-3}$ , a Young's modulus of 8.1 MPa, and a PhOH-removal rate of 500  $\text{mg L}^{-1}$ , or 0.76  $\text{mg (L h hydrogel g)}^{-1}$ .

**Acknowledgements** This work was partly supported by a Research for Promoting Technological Seeds 2007 grant (No. 12-095) from the Japan Science and Technology Agency and by a research promotion grant from the Conference for Reduction of Energy & Heat-trapping Gas in the Ube Industrial Complex (2005–2008). The authors are grateful to Kansai Paint Co., Ltd (Osaka) and Novozymes Japan Co., Ltd (Chiba) for providing ENTG 380 and DC 1002 CG, respectively.

## Compliance with ethical standards

**Conflict of interest** The authors declare no competing interests.

**Publisher's note** Springer Nature remains neutral with regard to jurisdictional claims in published maps and institutional affiliations.

## References

1. Yamasaki H, Nagasawa Y, Uchida N, Fukunaga K. Preparation of spherical photo-crosslinkable hydrogels having  $\beta$ -cyclodextrin powdery polymer and their application as immobilizing support for microbes. *KOBUNSHI RONBUNSHU Japanese. J Polym Sci Technol.* 2013;70:572–580.
2. Yamasaki H, Tokunaga H, Fukunaga K. Preparation of spherical PVA hydrogels bearing  $\beta$ -cyclodextrin and their application for immobilizing microbes. *KOBUNSHI RONBUNSHU Japanese. J Polym Sci Technol.* 2015;70:606–616.
3. Yamasaki H, Fukunaga K. Development of the environmental symbiosis material utilizing the property of cyclodextrin. *Jpn Environ Conser Eng* 2012;41:679–682.
4. Yamasaki, H., Takadera, T. & Matusmura, T. Japanese Patent No. 2014-5493123.
5. Yamasaki, H. Japanese Published Patent No. 2012-012582.
6. Takadera T, Yonehara Y. Study on continuous bio-ethanol fermentation process utilizing recombinant microorganism immobilized in/on supporting media composed of photo-curing materials. *Jpn Res Coat.* 2007;148:10–16.
7. Morita K, Izumida H. The removal technique of toxic substances from various drainage: Carrier for wastewater treatment “KP pearl”. *Jpn Sangyo Kankyo.* 2003;32:83–86.
8. Tanaka J. Nitrifying bacteria adhered on resinous carriers used in advanced sewage treatment system. *Jpn Res Coat.* 2002; 139:2–11.
9. Iida T. Denitrification of wastewater using microbial cells immobilized by synthetic polymers. *Jpn Biosci Ind.* 1998;56:675–678.
10. Iida T. Immobilization of bio-catalysts by photocrosslinkable resins. *J Jpn Soc Colour Mater.* 1990;63:153–162.
11. Iida T, Izumida H, Akagi Y, Sakamoto M. Continuous ethanol fermentation in molasses medium using zymomonas mobilis immobilized in photo-crosslinkable resin gel. *J Fermentation Bioeng.* 1993;75:32–35.
12. Sonomoto K, Tanaka A. Immobilization of biocatalysts with prepolymers. *Hakkokogaku.* 1983;61:153–172.
13. Yamasaki H, Odamura A, Makihata Y, Fukunaga K. Preparation of new photo-crosslinked  $\beta$ -cyclodextrin polymer beads. *Polym J.* 2017;49:377–383.
14. Yamaoka K, Kato M, Kamihara T. Control of cellular activity of dissimilatory nitrate reductase in escherichia coli. *Biosci Biotechnol Biochem.* 1994;58:995–997.

15. Yamasaki H, Tsujimura H, Sadaaki M, Shinagawa E, Sugimura Y, Fukunaga K. Treatment of super high concentration ammonium wastewater with immobilized aerobic nitrifying bacteria and stripping effects - Performance of nitrifying bacteria to tolerate a high concentration of ammonium sulfate. *Jpn Kagaku Kogaku Ronbunshu*. 2009;35:20–26.
16. Kimura, N. *Rhodococcus* biotechnology in biodegradation of nitroaromatic compounds. *Jpn J. Environ. Biotechnol.* 2007;7:19–25.
17. Crini G, Janus L, Morcellet M, Torri G, Morin N. Sorption properties toward substituted phenolic derivative in water using macroporous polyamines containing  $\beta$ -cyclodextrin. *J Appl Polym Sci.* 1999;73:2903–2910.